NACA

RESEARCH MEMORANDUM

A FINITE-STEP METHOD FOR THE CALCULATION OF SPAN LOADINGS OF UNUSUAL PLAN FORMS

By George S. Campbell

Langley Aeronautical Laboratory
Langley Field, Va.

NATIONAL ADVISORY COMMITTEE FOR AERONAUTICS

WASHINGTON
July 16, 1951

[redacted]

~~Security Information~~

N. 3469.
c.1

E R R A T U M

NACA RM L50L13

A FINITE-STEP METHOD FOR THE CALCULATION OF
SPAN LOADINGS OF UNUSUAL PLAN FORMS

By George S. Campbell

July 16, 1951

Page 8, equation (15): The sign preceding the first term on the right-hand side of this equation should be minus instead of plus so that the equation reads

$$p_{LE\bar{c}} = -\frac{(1 - K_b)^2\left[(1 + 2\lambda) - K_b(1 - \lambda)\right](\tan \Lambda_o - \tan \Lambda_i) + (1 + 2\lambda)\tan \Lambda_i}{3(1 + \lambda)} +$$

$$\frac{2}{3A}\left[1 - \frac{\lambda}{(1 + \lambda)^2}\right]$$

[redacted]

 [redacted]

NATIONAL ADVISORY COMMITTEE FOR AERONAUTICS

RESEARCH MEMORANDUM

A FINITE-STEP METHOD FOR THE CALCULATION OF SPAN LOADINGS OF UNUSUAL PLAN FORMS

By George S. Campbell

SUMMARY

The applicability of a well-known finite-step method to the calculation of subsonic spanwise load distribution, lift-curve slope, lateral center of pressure, and aerodynamic center of unusual plan forms has been investigated. Computing forms are presented to simplify calculation of span loadings for conventional swept, M plan-form, and W plan-form wings. Tables of the downwash in the plane of a yawed vortex are presented.

Comparison of loading results by using 20 steps with lifting-surface results indicated that the 20-step method generally overestimated the amount of loading at the wing tip. However, values of lift-curve slope, lateral center of pressure, aerodynamic center, and loading shape across the inboard three-quarter semispan obtained by using the 20-step method were generally in satisfactory agreement with lifting-surface results. Although use of an extra step at the wing tip provided some improvement in the load distribution near the tip, the over-all improvement did not appear to warrant the extra calculation time involved. For a representative W plan form, it was found that use of 20 steps provided a span loading that was essentially in agreement with 40-step results.

INTRODUCTION

The need to provide maximum structural strength and to eliminate undesirable aeroelastic phenomena, without sacrificing airplane performance or compromising acceptable stability and control characteristics at any speed, has stimulated interest in wings having very unusual plan forms. Comparisons of aerodynamic characteristics of such wings on a theoretical basis have met with some difficulties in the past, because the available wing theories generally have not been formulated in such a manner as to permit convenient and consistent applications of the theory to wings of widely different shapes. In the usual formulation of the theory, solutions based on Fourier series - and sometimes employing "middle functions" - are used in order to reduce the number of simultaneous

[redacted]

equations. Such solutions may be used profitably for wings having no abrupt changes in loading; however, for the more extreme cases, such as wings of extreme sweep or M and W plan forms, it is not clear that solution of the original simultaneous equations can be avoided.

In the present paper, solutions of span-load distributions, lift-curve slopes, lateral centers of pressure, and aerodynamic centers are obtained through a consistent application of generally accepted fundamentals of wing theory. The method involves the use of N horseshoe vortices placed along the lifting line and equating the downwash angle at the three-quarter chord to the local wing incidence to form N/2 equations in N/2 unknowns. Solutions of this type are somewhat cumbersome if performed with the usual type of manually operated computing equipment but are readily adaptable to relay-type digital computing machines.

The method used in the calculations is developed in detail. Computing forms and formulas facilitating solution for the span-load distribution and various aerodynamic parameters are presented. Applications of the basic 20-step method have been made for a series of wings having widely different plan forms, including unswept wings, swept wings, triangular wings, and M and W wings. Comparisons of results obtained by the present method and by currently available methods are made for some wings, and the effects of several modifications to the basic 20-step method have been illustrated.

SYMBOLS

Λ	sweep angle of quarter-chord line, positive for sweepback
A	aspect ratio (b^2/S)
λ	taper ratio (Tip chord/Root chord)
K_b	spanwise position of plan-form break for M or W wing
b	wing span
S	wing area
c	local streamwise chord
c_{av}	average chord (S/b)
$\bar{c}$	mean aerodynamic chord $\left(\frac{1}{S}\int_{-b/2}^{b/2} c^2 dy\right)$
t	fraction of chord at which control-point line is located
x, y	coordinates of a point on the wing surface with respect to axes of a given horseshoe vortex

x, P — longitudinal reference axes

p, q — coordinates of a point on the wing surface with respect to root quarter chord (see fig. 1)

y, Q — lateral reference axes

N — number of horseshoe vortices across total wing span

s — semiwidth of horseshoe vortex

$w(x, y)$ — downwash velocity at any point (x, y) in the plane of a horseshoe vortex, positive downward

$F(x, y)$ — downwash velocity at any point (x, y) caused by a rectangular horseshoe vortex of unit semiwidth and circulation strength equal to 4π (numerical values given in references 1 and 2)

$F_{\psi}(\psi, x, y)$ — downwash velocity at any point (x, y) caused by a yawed vortex of unit semiwidth and circulation strength equal to 4π (numerical values presented in table I)

F_{ν_n} — downwash coefficient; the downwash at any control point P_{ν} due to the nth horseshoe vortex

Γ — circulation strength

$\Gamma' = \dfrac{\Gamma}{\frac{b}{2}V\alpha}$

K — span-loading coefficient $\left(\dfrac{c_l c}{C_L c_{av}}\right)$

C_L — lift coefficient $\left(\dfrac{\text{Lift}}{\frac{1}{2}\rho V^2 S}\right)$

c_l — section lift coefficient $(2\Gamma/Vc)$

a_o — section lift-curve slope $(dc_l/d\alpha)$

α — angle of attack, radians

y_{cp} — lateral center-of-pressure location, percent semispan

a.c. — aerodynamic-center position, percent mean aerodynamic chord

ρ — mass density of air

V	free-stream velocity
M	Mach number

Subscripts and abbreviations:

n	number designating a particular horseshoe vortex, starting from left wing tip
ν	number designating a particular control point, starting from left wing tip
LE	leading edge
TE	trailing edge
i	inboard
o	outboard

Wing notation:

In this paper, wings are designated in two forms:

$\Lambda - A - \lambda$ for untapered wings and plan forms of intermediate taper

Λ°LE Δ for triangular wings, with Λ value indicating leading-edge sweep.

For example, 45-4-1 indicates a wing having 45° sweepback, aspect ratio 4, and taper ratio 1.0; and the designation 45°LE Δ indicates a triangular wing with leading-edge sweepback of 45°.

ANALYSIS

Basic Concepts

In order to calculate the subsonic span loading of an arbitrary wing, the wing may be replaced by a system of N horseshoe vortices along the quarter-chord line. An equal number of control points is taken along the three-quarter chord line, and the downwash velocity from the total vortex system is equated to the component of free-stream velocity normal to the wing chord at each control point. Application of this tangent-flow boundary condition for a symmetrical loading provides a set of $N/2$ simultaneous equations in the $N/2$ unknown circulation strengths across the semispan. Solution of this set of equations provides the span loading, and hence the lift slope and lateral center of pressure of an arbitrary plan form. The location of the wing aerodynamic center may be estimated using the assumption that the local aerodynamic center lies on the quarter chord (as in reference 3), although such an assumption is physically incorrect.

In the following derivation, a section lift-curve slope of 2π is implied as a consequence of the three-quarter-chord concept. The vortices placed along the lifting line are of the usual rectangular horseshoe type. (See fig. 1.)

Derivation of Method

The pattern of vortices and control points used to compute a 10-step span loading is illustrated in figure 1.

The downwash velocity in the plane of a rectangular horseshoe vortex is given by the expression

$$w(x,\ y) = \frac{\Gamma}{4\pi}\,\frac{F(x,\ y)}{s} \tag{1}$$

where

$$F(x,\ y) = -\frac{1}{x}\left[\frac{(y + 1)}{\sqrt{x^2 + (y + 1)^2}} - \frac{(y - 1)}{\sqrt{x^2 + (y - 1)^2}}\right] - \frac{1}{y - 1}\left[1 - \frac{x}{\sqrt{x^2 + (y - 1)^2}}\right] +$$

$$\frac{1}{y + 1}\left[1 - \frac{x}{\sqrt{x^2 + (y + 1)^2}}\right] \tag{2}$$

and the x and y distances are expressed in horseshoe semispans (see p. 159 of reference 4). The values of $F(x,\ y)$ are conveniently tabulated in references 1 and 2.

Distributing an even number N of horseshoe vortices having N control points across the wing span (fig. 1), the downwash velocity at any of the control points P_ν resulting from the N horseshoe vortices is

$$w\left(x_\nu,\ y_\nu\right) = \frac{N}{4\pi}\sum_{n=1}^{N}\left(\frac{\Gamma_n}{b/2}\right)F\left(x_\nu,\ y_\nu\right) \tag{3}$$

in which

$$\begin{aligned} x_\nu &= p_\nu - p_n \\ y_\nu &= q_\nu - q_n \end{aligned} \tag{4}$$

For cases of symmetrical loading and geometry, the downwash at any of the control points P_ν becomes

$$w(x_\nu, y_\nu) = \frac{N}{4\pi} \sum_{n=1}^{N/2} \left(\frac{\Gamma_n}{b/2}\right) F_{\nu_n} \tag{5}$$

with the coefficient F_{ν_n} being given in terms of geometrical distances measured in horseshoe semispans,

$$F_{\nu_n} = F\left[\left(p_\nu - p_n\right), \left(q_\nu - q_n\right)\right] + F\left[\left(p_\nu - p_n\right), \left(q_\nu + q_n\right)\right] \tag{6}$$

For a conventional swept wing (fig. 1), the longitudinal distance of any control point from the nth vortex is

$$\left(p_\nu - p_n\right) = \left[\left|q_n\right| - \left|q_\nu\right|\right] \tan \Lambda + \frac{2}{A(1 + \lambda)}\left[(1 - \lambda)\left|q_\nu\right| - N\right] \tag{7}$$

For unusual plan forms, these distances may be determined either graphically or analytically. An example of such a plan form is the W type shown in figure 2. The longitudinal distance for either M or W plan forms having linear taper over the semispan is

$$p_\nu - p_n = -\frac{2N}{A(1 + \lambda)} + K_b\left(\tan \Lambda_\nu - \tan \Lambda_n\right) -$$

$$\left|q_\nu\right| \left[\tan \Lambda_\nu - \frac{2(1 - \lambda)}{A(1 + \lambda)}\right] + \left|q_n\right| \tan \Lambda_n \tag{8}$$

with all distances expressed in horseshoe semispans.

For small angles, the tangent-flow boundary condition

$$w\left(x_\nu, y_\nu\right) = V \sin \alpha_\nu \cong V\alpha_\nu \tag{9}$$

may be applied at each control point to provide a set of N/2 simultaneous equations in the N/2 unknown circulation strengths from equation (5):

$$\left(\sum_{n=1}^{N/2} F_{\nu_n}\Gamma_n' = \frac{4\pi}{N}\frac{\alpha_\nu}{\alpha}\right)_{\nu=1,2,3,\ldots \frac{N}{2}} \tag{10}$$

For a symmetrical loading, solution of the set of N/2 simultaneous equations provides the unknown circulation strengths.

Calculation of Loading Parameters

A convenient form of the span-loading coefficient may be obtained from the relation

$$K = \frac{c_l c}{C_L c_{av}} = \frac{N}{2} \frac{\Gamma'}{\sum_{n=1}^{N/2} \Gamma_n'} \tag{11}$$

Lift-curve slope may be evaluated from the area under the symmetrical span loading. Thus,

$$\frac{dC_L}{d\alpha} = \frac{2A}{N} \sum_{n=1}^{N/2} \Gamma_n' \tag{12}$$

Lateral center of pressure is obtained from the formula

$$y_{cp} = \frac{200}{N} \sum_{n=1}^{N/2} \left|\frac{q_n}{b/2}\right| K_n \tag{13}$$

If the assumption is made that the local aerodynamic center lies on the quarter chord of streamwise wing sections, the aerodynamic center of a conventional swept wing is given in terms of lateral center of pressure by equation (1) of reference 3. Using the same assumption for an M or a W wing of linear taper, the aerodynamic center may be calculated from the $\frac{N}{2}$-step loading, using the relation

$$\text{a.c.} = \frac{100}{\bar{c}} \left\{ p_{LE\bar{c}} + \frac{2}{N} \sum_{\text{tip}}^{K_b} K_n \left[K_b \tan \Lambda_i + \left(|q_n| - K_b \right) \tan \Lambda_o \right] + \frac{2}{N} \sum_{K_b}^{\text{Root}} K_n |q_n| \tan \Lambda_i \right\} \tag{14}$$

with all distances conveniently expressed in wing semispans.

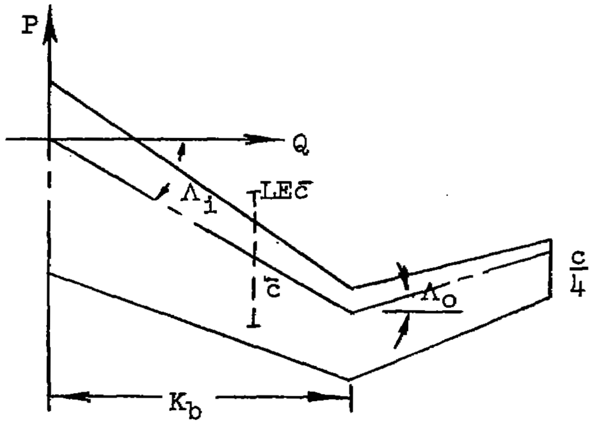

The chordwise location of the leading edge of the aerodynamic chord $p_{LE\bar{c}}$ (expressed in semispans) is given by the expression

$$p_{LE\bar{c}} = \frac{-(1 - K_b)^2\left[(1 + 2\lambda) - K_b(1 - \lambda)\right]\left(\tan\Lambda_o - \tan\Lambda_i\right) + (1 + 2\lambda)\tan\Lambda_i}{3(1 + \lambda)} + \frac{2}{3A}\left[1 - \frac{\lambda}{(1 + \lambda)^2}\right] \tag{15}$$

Use of Yawed Vortices

In the preceding analysis, rectangular vortices have been distributed along the lifting line of the wing. For swept wings, it would seem more reasonable to use vortices having bound elements lying along the quarter-chord line. The preceding development remains valid for such a case provided the downwash function F of equation (2) is replaced by the downwash function of a yawed vortex F_ψ.

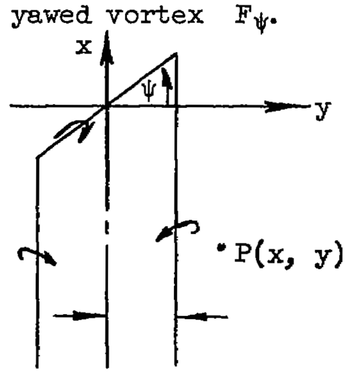

From a development similar to that of Glauert, this downwash function F_ψ may be shown to be

$$F_\psi(\psi, x, y) = \left(\frac{1}{y \sin\psi - x \cos\psi}\right)\left[\frac{(y + 1)\cos\psi + (x + \tan\psi)\sin\psi}{\sqrt{(y + 1)^2 + (x + \tan\psi)^2}} - \frac{(y - 1)\cos\psi + (x - \tan\psi)\sin\psi}{\sqrt{(y - 1)^2 + (x - \tan\psi)^2}}\right] + \frac{1}{y + 1}\left[1 - \frac{x + \tan\psi}{\sqrt{(y + 1)^2 + (x + \tan\psi)^2}}\right] - \frac{1}{y - 1}\left[1 - \frac{x - \tan\psi}{\sqrt{(y - 1)^2 + (x - \tan\psi)^2}}\right] \qquad (16)$$

The symbol F_ψ represents the downwash velocity at any point (x, y) caused by a yawed vortex of unit semiwidth and circulation strength equal to 4π, numerical values of this downwash function are presented in table I. Expressions for obtaining F_ψ at negative x positions along the vortex center line and for negative yaw angles are

$$F_\psi(\psi, -x, 0) = 4 - F_\psi(\psi, x, 0) \qquad (17)$$

$$F_\psi(-\psi, x, y) = F_\psi(\psi, x, -y) \qquad (18)$$

APPLICATIONS AND DISCUSSION

Use of Computing Forms

It has been found that use of 20 equal-width vortices (N = 20) has generally provided satisfactory loading solutions in about 9 hours, including solutions of the 10 simultaneous equations by use of the Crout method in conjunction with manually operated automatic computing machines. The use of a relay computer would reduce the time required to about 5 hours. Because of the practicability of such a 20-step system, a computing form (with illustrative values) for determining the loading coefficients of swept wings is presented in table II, and the coefficients have been placed in the expanded form of the 10 simultaneous equations (table III). A computing form for determining the loading coefficients of M or W plan-form wings is presented in table IV.

Comparison with Other Methods

Twenty-step loadings (N = 20) for seven plan forms are compared with Falkner's lifting-surface results of references 5 and 6 (126 vortices and six control points modified for center-line sweep discontinuity when indicated as 126-6 modified) and with results of the Weissinger method in figures 3 and 4. Five of the wings were untapered and the remaining two wings were of triangular plan form. In the following discussion, the Falkner lifting-surface solutions are taken as the best available standard of comparison. The aerodynamic-center position, as calculated by the Weissinger and 20-step method, is based on the assumption that the local center of pressure is located at the quarter chord.

The most noticeable disagreement of the 20-step method with both the Falkner and Weissinger solutions lies in the excess load indicated at the tip. However, for all plan forms shown, the 20-step lateral center of pressure was in no case greater than $1\frac{1}{2}$ percent semispan outboard of the lifting-surface value.

The 20-step lift-curve slopes for the untapered wings were generally in closer agreement with the lifting-surface results than were the Weissinger values, which were in all cases lower than the lift slopes of Falkner. For the triangular plan forms, the 20-step lift slopes were lower than Falkner's values, but the disagreement was no greater than that of the Weissinger method.

The agreement of the 20-step aerodynamic-center position with the lifting-surface value was generally satisfactory except at lower aspect ratios, particularly for the 45-1-1 wing (designation referring to sweep, aspect ratio, and taper ratio). This disagreement resulted primarily from the incorrect assumption that the local aerodynamic center lies at the quarter chord.

A particular case for which several theoretical solutions are available is presented in figure 4. In addition to the comparison with Falkner's lifting-surface calculation (fig. 4(a)), loadings obtained by four basically similar modified lifting-line methods are illustrated in figure 4(b) including the method of Schlichting (reference 7). First, it is seen that the agreement of Falkner's modified lifting-line loading with the lifting-surface result is reasonable, especially considering the calculation times involved. Secondly, for this moderately high combination of aspect ratio and sweepback, the center-loading dip appears to be exaggerated by the Weissinger method, and the lift slope is lowest for this method.

The theoretical methods of Falkner, Weissinger, and Schlichting all assume that the wing loading can be expressed in the form of a Fourier series. This assumption is not valid when there are rapid loading changes, and so the use of middle functions is frequently necessary. It is felt that since in the finite-step method of this paper no form whatever is assumed for the loading shape, involved treatment of localized dips and bumps is effectively side-stepped.

Modifications to 20-Step Method

Addition of extra step at tip.- Since use of 20 equal-width vortices generally provided an overestimate of the loading at the wing tip, the outboard step was replaced by two half-size vortices for three plan forms. To obtain downwash functions at uneven y values, the charts of reference 8 were used. Use of the extra tip step increased the over-all time of calculation by 40 percent and disrupted the routine of the computation. This latter factor makes computing more difficult and checking more involved.

The effect of the extra step (fig. 5) was to reduce the tip loading with little change in inboard load grading. Since the inboard load grading is the primary factor in the determination of theoretical downwash, it is seen that on the basis of these limited results, use of an extra step at the tip would have negligible effect on downwash calculations.

In comparing these loadings with those of Falkner (figs. 3(d) and 4(a)), it is seen that use of the extra tip step did not effect any marked improvement in the agreement of over-all loading shape or aerodynamic parameters with lifting-surface results.

Effect of yawed vortices and number of steps.- The effect of yawed vortices on a calculated span loading is negligible if the control points are located a sufficiently large number of horseshoe semiwidths behind the lifting line so that yawing of the bound vortex does not modify the loading coefficients F_{ν_n} to any important degree. However, there are several factors which would tend to increase the downwash contribution of the bound vortices: reduced number of steps, increased aspect ratio, increased sweep, decreased taper ratio, and/or reduced section lift-curve slope. Although no consistent investigation of the aforementioned factors has been made, limited results using yawed vortices are presented in figure 6.

For a moderately high aspect ratio, it is seen that the use of yawed vortices had a negligible effect on the 20-step span loading (fig. 6(a)). However, the use of 10 yawed vortices provided a better estimate of the 20-step loading than did an equal number of rectangular vortices. As would be expected, the effect of yawed vortices on span loading was negligible for low-aspect-ratio wings. (See figs. 6(b) and 6(c).)

While the lift slopes obtained by using yawed vortices were generally different from the values for rectangular vortices, no consistent effect was observed and, for all cases calculated, the difference was less than 2 percent.

In addition to the results presented, it has been found from loading calculations for several untapered 45° sweptback wings from aspect ratios of 1.3 to 5.2 that 10 rectangular vortices were sufficient to provide lift slopes that were in close agreement with both experimental values and with the modified lifting-line results of reference 9.

Effect of section lift-curve slope.- A commonly used method for calculating the incompressible aerodynamic characteristics of wings having a section lift-curve slope other than 2π involves a change in the control-point location in the ratio of $a_o/2\pi$. (See reference 9.) A limited study of the effects of a_o change on the spanwise load distribution has been made by utilizing the aforementioned control-point concept and the methods of the present paper, and the results are presented in figure 7. A change in a_o of 10 percent produced only minor changes in the spanwise load distributions. A more substantial effect on load distribution is evident, however, for a $33\frac{1}{3}$-percent reduction in a_o and the computing sheets (for example, table II) have been set up to include the effect of section lift slope based on the control-point concept. The problem of the proper airfoil section to use in determining a_o is discussed briefly in reference 9. The effects of section lift slope on wing lift slope are also presented in figure 7 and the effects shown can be computed from equation (8) of reference 10.

Additional applications of method.- The versatility of the finite-step method makes it particularly useful for unusual problems, such as M and W plan-form calculations. Moreover, the method is readily adaptable to the calculation of loading estimates for twisted and cambered wings, estimation of the effect of elastic deformation on aerodynamic parameters, loading calculations for coupled aircraft, and problems requiring a method that may be readily understood and adapted.

Results for an M and a W Plan Form

An example of a plan form for which the use of the finite-step method is particularly suited is the wing of M or W plan form. The incompressible loadings for the sweptback M and W wings of figure 8 are presented in figure 9(a). The Prandtl-Glauert transformation has been used to obtain the compressible loadings (Mach number of 0.7) for these same wings (fig. 9(b)). The calculated effect of Mach number on load distribution was relatively small (at $M = 0.7$), while the lift-curve slopes of all three wings were increased by nearly the same percentage with increase in Mach number. Moreover, the lift slopes of the M and W wings were essentially equal to the values for the comparable swept-back wing at both zero and 0.7 Mach numbers.

The W wing of figure 8 has been chosen to illustrate the effect of number of steps and of yawed vortices on span loading. It is seen that the calculated loading at the tip is reduced slightly by the use of 40 steps in place of 20. (See fig. 10.) The over-all change in loading shape and aerodynamic parameters was negligible for the case investigated. The span loadings obtained using rectangular and yawed vortices are also presented; the over-all accuracy was essentially equal using yawed or unyawed vortices.

CONCLUDING REMARKS

Comparison of loading results by using 20 steps with lifting-surface results indicated that the 20-step method generally overestimated the amount of loading at the wing tip. However, values of lift-curve slope, lateral center of pressure, aerodynamic center, and loading shape across the inboard three-quarter semispan by using the 20-step method were generally in satisfactory agreement with lifting-surface results. Although use of an extra step at the wing tip provided some improvement in the load distribution near the tip, the over-all improvement did not appear to warrant the extra calculation time involved. For a representative W plan form, it was found that use of 20 steps provided a span loading that was essentially in agreement with 40-step results.

Langley Aeronautical Laboratory
National Advisory Committee for Aeronautics
Langley Field, Va.

REFERENCES

1. Staff of the Mathematics Division: Tables of Complete Downwash Due to a Rectangular Vortex. Rep. No. 10754, British A.R.C., July 21, 1947.

2. Van Dorn, Nicholas H., and DeYoung, John: A Comparison of Three Theoretical Methods of Calculating Span Load Distribution on Swept Wings. NACA TN 1476, 1947.

3. DeYoung, John: Theoretical Additional Span Loading Characteristics of Wings with Arbitrary Sweep, Aspect Ratio, and Taper Ratio. NACA TN 1491, 1947.

4. Glauert, H.: The Elements of Aerofoil and Airscrew Theory. Second ed., Cambridge Univ. Press, 1948.

5. Falkner, V. M.: Calculated Loadings Due to Incidence of a Number of Straight and Swept-Back Wings. Rep. No. 11,542, British A.R.C., June 5, 1948.

6. Falkner, V. M.: The Solution of Lifting Plane Problems by Vortex Lattice Theory. Rep. No. 10,895, British A.R.C., Sept. 29, 1947.

7. Schlichting, H., and Kahlert, W.: Calculation of Lift Distribution of Swept Wings. Rep. No. Aero. 2297, British R.A.E., Oct. 1948.

8. Gray, W. L., and Schenk, K. M.: A Matrix Solution for the Steady State Aeroelastic Loading on Wings (Rough Draft). Document No. D 10624, Boeing Aircraft Co., March 24, 1950.

9. DeYoung, John, and Harper, Charles W.: Theoretical Symmetric Span Loading at Subsonic Speeds for Wings Having Arbitrary Plan Form. NACA Rep. 921, 1948.

10. Polhamus, Edward C.: A Simple Method of Estimating the Subsonic Lift and Damping in Roll of Sweptback Wings. NACA TN 1862, 1949.

TABLE I.- DOWNWASH FUNCTION $F_\psi(\psi, x, y)$ FOR YAWED VORTICES

$$F_\psi(\psi, x, y) = \left[\frac{1}{y \sin \psi - x \cos \psi}\right]\left[\frac{(y + 1)\cos \psi + (x + \tan \psi)\sin \psi}{\sqrt{(y + 1)^2 + (x + \tan \psi)^2}} - \frac{(y - 1)\cos \psi + (x - \tan \psi)\sin \psi}{\sqrt{(y - 1)^2 + (x - \tan \psi)^2}}\right] + \frac{1}{y + 1}\left[1 - \frac{(x + \tan \psi)}{\sqrt{(y + 1)^2 + (x + \tan \psi)^2}}\right] - \frac{1}{y - 1}\left[1 - \frac{(x - \tan \psi)}{\sqrt{(y - 1)^2 + (x - \tan \psi)^2}}\right]$$

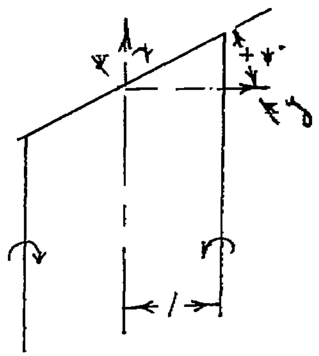

$$F_\psi(\psi, -x, 0) = 4 - F_\psi(\psi, x, 0)$$

$$F(-\psi, x, y) = F_\psi(\psi, x, -y)$$

DISTANCES EXPRESSED IN VORTEX SEMIWIDTHS

x	$F_\psi(\psi, x, y)$ for ψ =			x	$F_\psi(\psi, x, y)$ for ψ =		
	30°	45°	60°		30°	45°	60°
	y = 0				y = 0		
0.50	-2.9458	-3.8416	-6.0653	0.57	-2.4246	-3.1754	-5.0929
.51	-2.8618	-3.7347	-5.9098	.58	-2.3613	-3.0939	-4.9734
.52	-2.7813	-3.6321	-5.7604	.59	-2.3003	-3.0154	-4.8580
.53	-2.7041	-3.5335	-5.6167	.60	-2.2416	-2.9397	-4.7465
.54	-2.6300	-3.4387	-5.4784	.61	-2.1851	-2.8666	-4.6387
.55	-2.5588	-3.3476	-5.3452	.62	-2.1305	-2.7961	-4.5344
.56	-2.4904	-3.2599	-5.2168	.63	-2.0779	-2.7279	-4.4335

TABLE I.- DOWNWASH FUNCTION $F_\psi(\psi, x, y)$ FOR YAWED VORTICES - Continued

x	$F_\psi(\psi, x, y)$ for ψ =		
	30°	45°	60°
y = 0			
0.64	-2.0272	-2.6620	-4.3359
.65	-1.9781	-2.5982	-4.2413
.66	-1.9308	-2.5366	-4.1496
.67	-1.8851	-2.4769	-4.0607
.68	-1.8409	-2.4192	-3.9744
.70	-1.7567	-2.3091	-3.8095
.72	-1.6780	-2.2056	-3.6540
.74	-1.6041	-2.1083	-3.5071
.76	-1.5348	-2.0166	-3.3682
.78	-1.4696	-1.9302	-3.2365
.80	-1.4082	-1.8487	-3.1117
.82	-1.3504	-1.7716	-2.9932
.84	-1.2959	-1.6987	-2.8806
.86	-1.2444	-1.6297	-2.7734
.88	-1.1957	-1.5643	-2.6712
.90	-1.1497	-1.5023	-2.5739
.92	-1.1061	-1.4435	-2.4810
.94	-1.0649	-1.3876	-2.3923
.96	-1.0257	-1.3345	-2.3074
.98	-.9886	-1.2841	-2.2263
1.00	-.9533	-1.2361	-2.1486
1.05	-.8725	-1.1259	-1.9684
1.10	-.8011	-1.0281	-1.8058
1.15	-.7376	-.9412	-1.6588
1.20	-.6811	-.8637	-1.5255
1.25	-.6306	-.7944	-1.4043
1.30	-.5853	-.7323	-1.2939
1.35	-.5445	-.6766	-1.1931
1.40	-.5077	-.6265	-1.1011
1.50	-.4441	-.5404	-.9399
1.60	-.3915	-.4699	-.8047
1.80	-.3103	-.3632	-.5962
2.00	-.2517	-.2882	-.4495
2.40	-.1749	-.1935	-.2725
3.00	-.1118	-.1197	-.1505
4.00	-.0628	-.0653	-.0743
6.00	-.0278	-.0283	-.0300
10.00	-.0100	-.0101	-.0103
20.00	-.0025	-.0025	-.0025
40.00	-.0006	-.0006	-.0006
60.00	-.0003	-.0003	-.0003

x	$F_\psi(\psi, x, y)$ for ψ =		
	30°	45°	60°
y = 2			
-60.00	-1.3331	-1.3331	-1.3331
-20.00	-1.3309	-1.3308	-1.3308
-10.00	-1.3236	-1.3236	-1.3234
-6.00	-1.3078	-1.3076	-1.3067
-4.00	-1.2813	-1.2808	-1.2783
-3.00	-1.2513	-1.2509	-1.2469
-2.00	-1.1922	-1.1937	-1.1900
-1.50	-1.1410	-1.1463	-1.1462
-1.20	-1.0990	-1.1087	-1.1131
-1.00	-1.0648	-1.0787	-1.0878
-.80	-1.0244	-1.0441	-1.0595
-.60	-.9771	-1.0043	-1.0280
-.40	-.9217	-.9586	-.9929
-.30	-.8908	-.9333	-.9740
-.20	-.8576	-.9063	-.9540
-.10	-.8223	-.8774	-.9329
.00	-.7847	-.8467	-.9107
.10	-.7453	-.8142	-.8873
.20	-.7042	-.7798	-.8628
.30	-.6618	-.7436	-.8370
.40	-.6188	-.7058	-.8099
.60	-.5333	-.6265	-.7518
.80	-.4528	-.5447	-.6886
1.00	-.3813	-.4648	-.6207
1.20	-.3206	-.3913	-.5494
1.50	-.2488	-.2993	-.4409
2.00	-.1691	-------	-.2836
3.00	-.0897	-.0973	-.1220
4.00	-.0546	-.0574	-.0657
6.00	-.0260	-.0266	-.0282
10.00	-.0097	-.0098	-.0100
20.00	-.0025	-.0025	-.0025
60.00	-.0003	-.0003	-.0003
y = -2			
-60.00	-1.3331	-1.3331	-1.3331
-20.00	-1.3308	-1.3308	-1.3308
-10.00	-1.3236	-1.3235	-1.3233
-6.00	-1.3074	-1.3068	-1.3051
-4.00	-1.2787	-1.2760	-1.2677
-3.00	-1.2436	-1.2361	-1.2114

NACA

TABLE I.- DOWNWASH FUNCTION $F_\psi(\psi, x, y)$ FOR YAWED VORTICES - Continued

x	$F_\psi(\psi, x, y)$ for ψ =		
	30°	45°	60°
	y = -2		
-2.00	-1.1642	-1.1381	-1.0497
-1.50	-1.0845	-1.0340	-.8924
-1.20	-1.0128	-.9420	-.7840
-1.00	-.9521	-.8685	-.7126
-.80	-.8806	-.7887	-.6447
-.60	-.8001	-.7069	-.5815
-.40	-.7145	-.6275	-.5235
-.30	-.6715	-.5897	-.4964
-.20	-.6292	-.5536	-.4706
-.10	-.5880	-.5192	-.4460
.00	-.5486	-.4866	-.4226
.10	-.5111	-.4559	-.4005
.20	-.4757	-.4271	-.3794
.30	-.4425	-.4000	-.3594
.40	-.4116	-.3747	-.3404
.60	-.3562	-.3290	-.3053
.80	-.3089	-.2892	-.2738
1.00	-.2686	-.2546	-.2455
1.20	-.2343	-.2247	-.2202
1.50	-.1923	-.1870	-.1872
2.00	-.1412	-.1396	-.1433
3.00	-.0820	-.0824	-.0864
4.00	-.0520	-.0525	-.0551
6.00	-.0255	-.0257	-.0266
10.00	-.0097	-.0097	-.0099
20.00	-.0025	-.0025	-.0025
60.00	-.0003	-.0003	-.0003
	y = 4		
-60.00	-0.2664	-0.2664	-0.2664
-10.00	-.2577	-.2577	-.2576
-5.00	-.2395	-.2395	-.2391
-3.00	-.2172	-.2176	-.2175
-2.00	-.1980	-.1991	-.1999
-1.00	-.1715	-.1737	-.1765
-.20	-.1454	-.1486	-.1535
.20	-.1314	-.1351	-.1409
1.00	-.1038	-.1077	-.1147
2.00	-.0742	-.0773	-.0838
3.00	-.0526	-.0546	-.0592
5.00	-0.0280	-0.0287	-0.0304
10.00	-.0090	-.0091	-.0092
20.00	-.0024	-.0024	-.0024
60.00	-.0003	-.0003	-.0003
	y = -4		
-60.00	-0.2664	-0.2664	-0.2664
-10.00	-.2577	-.2576	-.2574
-5.00	-.2386	-.2379	-.2362
-3.00	-.2141	-.2121	-.2075
-2.00	-.1925	-.1894	-.1828
-1.00	-.1629	-.1590	-.1519
-.20	-.1353	-.1316	-.1258
.20	-.1213	-.1180	-.1132
1.00	-.0952	-.0930	-.0902
2.00	-.0687	-.0676	-.0667
3.00	-.0495	-.0491	-.0491
5.00	-.0272	-.0272	-.0275
10.00	-.0089	-.0089	-.0090
20.00	-.0024	-.0024	-.0024
60.00	-.0003	-.0003	-.0003
	y = 6		
-60.00	-0.1140	-0.1140	-0.1140
-20.00	-.1119	-.1119	-.1119
-10.00	-.1064	-.1064	-.1063
-4.00	-.0896	-.0898	-.0898
-2.50	-.0801	-.0804	-.0807
-1.00	-.0676	-.0681	-.0689
.00	-.0581	-.0588	-.0599
1.00	-.0484	-.0491	-.0505
2.50	-.0354	-.0360	-.0373
4.00	-.0254	-.0258	-.0267
10.00	-.0080	-.0080	-.0082
20.00	-.0023	-.0024	-.0024
60.00	-.0003	-.0003	-.0003

NACA

TABLE I.- DOWNWASH FUNCTION $F_\psi'(\psi, x, y)$ FOR YAWED VORTICES - Continued

x	$F_\psi(\psi, x, y)$ for ψ =		
	30°	45°	60°
$y = -6$			
-60.00	-0.1140	-0.1140	-0.1140
-20.00	-.1119	-.1119	-.1119
-10.00	-.1063	-.1063	-.1061
-4.00	-.0889	-.0885	-.0876
-2.50	-.0789	-.0783	-.0770
-1.00	-.0659	-.0651	-.0638
.00	-.0562	-.0555	-.0544
1.00	-.0467	-.0461	-.0454
2.50	-.0341	-.0339	-.0336
4.00	-.0246	-.0245	-.0245
10.00	-.0079	-.0079	-.0080
20.00	-.0023	-.0023	-.0024
60.00	-.0003	-.0003	-.0003
$y = 8$			
-60.00	-0.0632	-0.0632	-0.0632
-15.00	-.0598	-.0598	-.0598
-7.00	-.0528	-.0529	-.0528
-3.00	-.0432	-.0433	-.0434
-1.00	-.0360	-.0362	-.0365
.00	-.0320	-.0322	-.0326
1.00	-.0280	-.0283	-.0287
3.00	-.0207	-.0209	-.0213
7.00	-.0108	-.0109	-.0111
15.00	-.0037	-.0037	-.0037
60.00	-.0003	-.0003	-.0003
$y = -8$			
-60.00	-0.0632	-0.0632	-0.0632
-15.00	-.0598	-.0598	-.0598
-7.00	-.0527	-.0526	-.0524
-3.00	-.0428	-.0426	-.0422
-1.00	-.0355	-.0352	-.0348
.00	-.0315	-.0312	-.0309
1.00	-.0275	-.0273	-.0270
3.00	-.0203	-.0202	-.0200
7.00	-.0106	-.0106	-.0106
15.00	-.0037	-.0037	-.0037
60.00	-.0003	-.0003	-.0003

x	$F_\psi(\psi, x, y)$ for ψ =		
	30°	45°	60°
$y = 10$			
-60.00	-0.0401	-0.0401	-0.0401
-15.00	-.0370	-.0370	-.0370
-5.00	-.0294	-.0294	-.0294
1.00	-.0223	-.0224	-.0225
1.00	-.0183	-.0184	-.0185
5.00	-.0112	-.0112	-.0114
15.00	-.0034	-.0034	-.0034
60.00	-.0003	-.0003	-.0003
$y = -10$			
-60.00	-0.0401	-0.0401	.0401
-15.00	-.0370	-.0370	-.0370
-5.00	-.0292	-.0292	-.0290
-1.00	-.0221	-.0220	-.0219
1.00	-.0181	-.0180	-.0179
5.00	-.0110	-.0110	-.0110
15.00	-.0034	-.0034	-.0034
60.00	-.0003	-.0003	-.0003
$y = 12$			
-60.00	-0.0277	-0.0277	-0.0277
-15.00	-.0249	-.0249	-.0249
-5.00	-.0194	-.0194	-.0195
.00	-.0140	-.0141	-.0142
5.00	-.0086	-.0087	-.0087
15.00	-.0031	-.0031	-.0031
60.00	-.0003	-.0003	-.0003
$y = -12$			
-60.00	-0.0277	-0.0277	-0.0277
-15.00	-.0249	-.0249	-.0249
-5.00	-.0194	-.0193	-.0192
.00	-.0139	-.0139	-.0138
5.00	-.0085	-.0085	-.0085
15.00	-.0030	-.0030	-.0030
60.00	-.0003	-.0003	-.0003

NACA

TABLE I.- DOWNWASH FUNCTION $F_\psi(\psi, x, y)$ FOR YAWED VORTICES - Concluded

x	$F_\psi(\psi, x, y)$ for ψ =		
	30°	45°	60°
	y = 14		
-60.00	-0.0202	-0.0202	-0.0202
-10.00	-.0162	-.0162	-.0162
-3.00	-.0124	-.0125	-.0125
3.00	-.0081	-.0081	-.0082
10.00	-.0043	-.0043	-.0043
60.00	-.0003	-.0003	-.0003
	y = -14		
-60.00	-0.0202	-0.0202	-0.0202
-10.00	-.0162	-.0162	-.0162
-3.00	-.0124	-.0124	-.0123
3.00	-.0081	-.0081	-.0080
10.00	-.0043	-.0043	-.0043
60.00	-.0003	-.0003	-.0003
	y = 16		
-60.00	-0.0154	-0.0154	-0.0154
-10.00	-.0120	-.0120	-.0120
-2.00	-.0088	-.0088	-.0089
2.00	-.0069	-.0069	-.0069
10.00	-.0037	-.0037	-.0037
40.00	-.0006	-.0006	-.0006
	y = -16		
-60.00	-0.0154	-0.0154	-0.0154
-10.00	-.0120	-.0120	-.0120
-2.00	-.0088	-.0088	-.0088
2.00	-.0068	-.0068	-.0068
10.00	-.0037	-.0037	-.0037
40.00	-.0006	-.0006	-.0006

x	$F_\psi(\psi, x, y)$ for ψ =		
	30°	45°	60°
	y = 18		
-60.00	-0.0121	-0.0121	-0.0121
-10.00	-.0092	-.0092	-.0092
.00	-.0062	-.0062	-.0062
10.00	-.0032	-.0032	-.0032
40.00	-.0005	-.0005	-.0005
	y = -18		
-60.00	-0.0121	-0.0121	-0.0121
-10.00	-.0092	-.0092	-.0092
.00	-.0062	-.0062	-.0062
10.00	-.0032	-.0032	-.0032
40.00	-.0005	-.0005	-.0005
	y = 20		
-60.00	-0.0098	-0.0098	-0.0098
-10.00	-.0073	-.0073	-.0073
.00	-.0050	-.0050	-.0050
10.00	-.0028	-.0028	-.0028
40.00	-.0005	-.0005	-.0005
	y = -20		
-60.00	-0.0098	-0.0098	-0.0098
-10.00	-.0073	-.0072	-.0072
.00	-.0050	-.0050	-.0050
10.00	-.0028	-.0028	-.0028
40.00	-.0005	-.0005	-.0005

NACA

TABLE II.- COMPUTING FORM FOR 20-STEP LOADING COEFFICIENTS OF A SWEPT WING BY USING ILLUSTRATED YAWED VORTICES

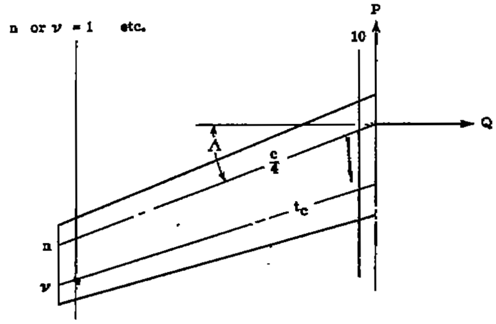

$t - \frac{1}{4} = \frac{a_0}{4\pi} = \frac{1}{2}$

$\Lambda = 45^\circ$

$A = 6$

$\lambda = 0.6$

$a_0 = 2\pi$

$(1) = \frac{4\left(t - \frac{1}{4}\right)}{A(1 + \lambda)} = 0.20833$

[All values expressed in horseshoe semiwidths]

(1) ν	(2) n	(3) q_ν	(4) q_n	(5) $q_\nu - q_n = \lvert(4)\rvert - \lvert(3)\rvert$	(6) (5) tan Λ (1)	(7) (1 − λ) × (3)	(8) (7) − 20	(9) (1) × (8)	(10) $p_\nu - p_n$ (6) + (9)	(11) $q_\nu + q_n$ (3) + (4)	(12) Left F_ψ(45°, (10), (5))	(13) Right F_ψ(45°, (10), −(11))	(14) $F_{\nu n}$ (12) + (13)
											Table I		
1	1	-19	-19	0		7.6	-12.4	-2.5833	-2.5833	-38	4.165	-0.001	4.164
	2		-17	-2					-4.5833	-36	-1.290	-.002	-1.292
	3		-15	-4					-6.5833	-34	-.248	-.002	-.250
	4		-13	-6					-8.5833	-32	-.104	-.002	-.106
	5		-11	-8					-10.5833	-30	-.057	-.003	-.060
	6		-9	-10					-12.5833	-28	-.036	-.004	-.040
	7		-7	-12					-14.5833	-26	-.025	-.004	-.029
	8		-5	-14					-16.5833	-24	-.018	-.005	-.023
	9		-3	-16					-18.5833	-22	-.014	-.007	-.021
	10		-1	-18					-20.5833	-20	-.011	-.008	-.019
2	1	-17	-19	2		6.8	-13.2	-2.7500	-0.7500	-36	-1.035	-0.002	-1.037
	2		-17	0					-2.7500	-34	4.144	-.002	4.142
	3		-15	-2					-4.7500	-32	-1.293	-.002	-1.295
	4		-13	-4					-6.7500	-30	-.248	-.003	-.251
	5		-11	-6					-8.7500	-28	-.104	-.003	-.107
	6		-9	-8					-10.7500	-26	-.057	-.004	-.061
	7		-7	-10					-12.7500	-24	-.036	-.005	-.041
	8		-5	-12					-14.7500	-22	-.025	-.006	-.031
	9		-3	-14					-16.7500	-20	-.018	-.008	-.026
	10		-1	-16					-18.7500	-18	-.014	-.010	-.024
10	1	-1	-19	18		0.4	-19.6	-4.0833	13.9167	-20	-0.002	-0.002	-0.004
	2		-17	16					11.9167	-18	-.003	-.003	-.006
	3		-15	14					9.9167	-16	-.004	-.004	-.008
	4		-13	12					7.9167	-14	-.007	-.005	-.012
	5		-11	10					5.9167	-12	-.010	-.008	-.018
	6		-9	8					3.9167	-10	-.018	-.013	-.031
	7		-7	6					1.9167	-8	-.040	-.024	-.064
	8		-5	4					-.0833	-6	-.145	-.066	-.211
	9		-3	2					-2.0833	-4	-1.200	-.200	-1.400
	10		-1	0					-4.0833	-2	4.063	-1.282	2.781

[1]Same as column 5, Λ = 45°

NACA

[redacted]

TABLE III.- ILLUSTRATIVE EXAMPLE OF 20-STEP LOADING SOLUTION USING YAWED VORTICES

$\Lambda = 45^\circ$, $A = 6$, $\lambda = 0.6$, $a_0 = 2\pi$

ν	Γ'_1	Γ'_2	Γ'_3	Γ'_4	Γ'_5	Γ'_6	Γ'_7	Γ'_8	Γ'_9	Γ'_{10}	=
1	4.164	-1.292	-0.250	-0.106	-0.060	-0.040	-0.029	-0.023	-0.021	-0.019	0.628318
2	-1.037	4.142	-1.295	-.251	-.107	-.061	-.041	-.031	-.026	-.024	.628318
3	-.107										.628318
4	-.035										.628318
5	-.017										.628318
6	-.012										.628318
7	-.008										.628318
8	-.006										.628318
9	-.005										.628318
10	-.004	-.006	-.008	-.012	-.018	-.031	-.064	-.211	-1.400	2.781	.628318

$$\frac{dC_L}{d\alpha} = \frac{A}{10}\sum_{n=1}^{10}\Gamma'_n$$

$$= \underline{3.548}$$

$$y_{cp} = 10\sum_{n=1}^{10}\frac{|y_n|}{b/2}K_n$$

$$= \underline{46.66}$$

$$\text{a.c.} = \underline{27.44}$$

equation (1) of TN 1491

$$K = \frac{c_l c}{C_L c_{av}} = \frac{10\,\Gamma'}{\sum_{n=1}^{10}\Gamma'_n}$$

$K_1 = \underline{0.658}$	$K_6 = \underline{1.087}$
$K_2 = \underline{0.854}$	$K_7 = \underline{1.106}$
$K_3 = \underline{0.951}$	$K_8 = \underline{1.112}$
$K_4 = \underline{1.004}$	$K_9 = \underline{1.102}$
$K_5 = \underline{1.056}$	$K_{10} = \underline{1.075}$

$\Gamma'_1 = \underline{0.3860}$	$\Gamma'_6 = \underline{0.6429}$
$\Gamma'_2 = \underline{0.5049}$	$\Gamma'_7 = \underline{0.6542}$
$\Gamma'_3 = \underline{0.5624}$	$\Gamma'_8 = \underline{0.6578}$
$\Gamma'_4 = \underline{0.5936}$	$\Gamma'_9 = \underline{0.6516}$
$\Gamma'_5 = \underline{0.6241}$	$\Gamma'_{10} = \underline{0.6358}$

$$\Gamma' = \frac{\Gamma}{\frac{b}{2}V\alpha}$$

$$\sum_{n=1}^{10}\Gamma'_n = \underline{5.913}$$

NACA

[redacted]

TABLE IV.- COMPUTING FORM FOR 20-STEP LOADING COEFFICIENTS OF M OR W WINGS;

USING RECTANGULAR VORTICES

Illustrated for W wing

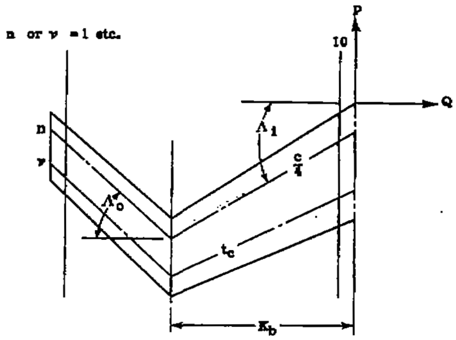

$\tan\Lambda_{1\to5} = \underline{-1}$

$\tan\Lambda_{6\to10} = \underline{+1}$

$A = \underline{6}$

$\lambda = \underline{0.6}$

$K_b = \underline{10}$

$a_o = \underline{2\pi}$

$t - \frac{1}{4} = \frac{a_o}{4\pi} = \underline{\frac{1}{2}}$

$(\mathrm{I}) = \frac{80\left(t - \frac{1}{4}\right)}{A(1+\lambda)} = \underline{4.16667}$

$(\mathrm{II}) = \frac{4(1-\lambda)\left(t - \frac{1}{4}\right)}{A(1+\lambda)} = \underline{0.08333}$

All values are expressed in horseshoe semiwidths

Columns indicated show repetition for equal n

(1) ν	(2) n	(3) $\tan\Lambda_\nu$	(4) $\tan\Lambda_n$	(5) (3) - (II)	(6) K_b (3) - (4)	(7) q_ν	(8) q_n	(9) (5) × |(7)|	(10) (4) × |(8)|	(11) -(I)-(9)	(12) $p_\nu - p_n$ (6)+(10)+(11)	(13) $q_\nu - q_n$ (7)-(8)	(14) $q_\nu + q_n$ (7)+(8)	(15) Left F((12),(13))	(16) Right F((12),(14))	(17) $F_{\nu n}$ (15)+(16)
1	1	-1	-1	-1.0833	0	-19	-19	-20.5833	-19	16.4167	-2.5833	0	-38	4.145	-0.001	4.144
	2						-17		-17		-.5833	-2	-36	-.905	-.002	-.907
	3						-15		-15		1.4167	-4	-34	-.086	-.002	-.088
	4						-13		-13		3.4167	-6	-32	-.028	-.002	-.030
	5						-11		-11		5.4167	-8	-30	-.014	-.002	-.016
	6		+1		-20		-9		9		5.4167	-10	-28	-.011	-.002	-.013
	7						-7		7		3.4167	-12	-26	-.010	-.003	-.013
	8						-5		5		1.4167	-14	-24	-.009	-.003	-.012
	9						-3		3		-.5833	-16	-22	-.008	-.004	-.012
	10						-1		1		-2.5833	-18	-20	-.007	-.006	-.013
2	1	-1	-1	-1.0833	0	-17	-19	-18.4167	-19	14.2500	-4.7500	2	-36	-1.294	-0.002	-1.296
	2						-17		-17		-2.7500	0	-34	4.128	-.002	4.126
	3						-15		-15		-.7500	-2	-32	-.959	-.002	-.961
	4						-13		-13		1.2500	-4	-30	-.091	-.002	-.093
	5						-11		-11		3.2500	-6	-28	-.029	-.002	-.031
	6		+1		-20		-9		9		3.2500	-8	-26	-.020	-.003	-.023
	7						-7		7		1.2500	-10	-24	-.018	-.003	-.021
	8						-5		5		-.7500	-12	-22	-.015	-.004	-.019
	9						-3		3		-2.7500	-14	-20	-.012	-.006	-.018
	10						-1		1		-4.7500	-16	-18	-.010	-.008	-.018
10	1	+1	-1	0.9167	20	-1	-19	0.9167	-19	-6.0833	-4.0833	18	-20	-0.008	-0.006	-0.014
	2						-17		-17		-2.0833	16	-18	-.009	-.007	-.016
	3						-15		-15		-.0833	14	-16	-.011	-.008	.019
	4						-13		-13		1.9167	12	-14	-.012	-.009	-.021
	5						-11		-11		3.9167	10	-12	-.013	-.010	-.023
	6		+1		0		-9		9		3.9167	8	-10	-.018	-.013	-.031
	7						-7		7		1.9167	6	-8	-.039	-.024	-.063
	8						-5		5		-.0833	4	-6	-.136	-.058	-.194
	9						-3		3		-2.0833	2	-4	-1.192	-.198	-1.390
	10						-1		1		-4.0833	0	-2	4.059	-1.288	2.776

NACA

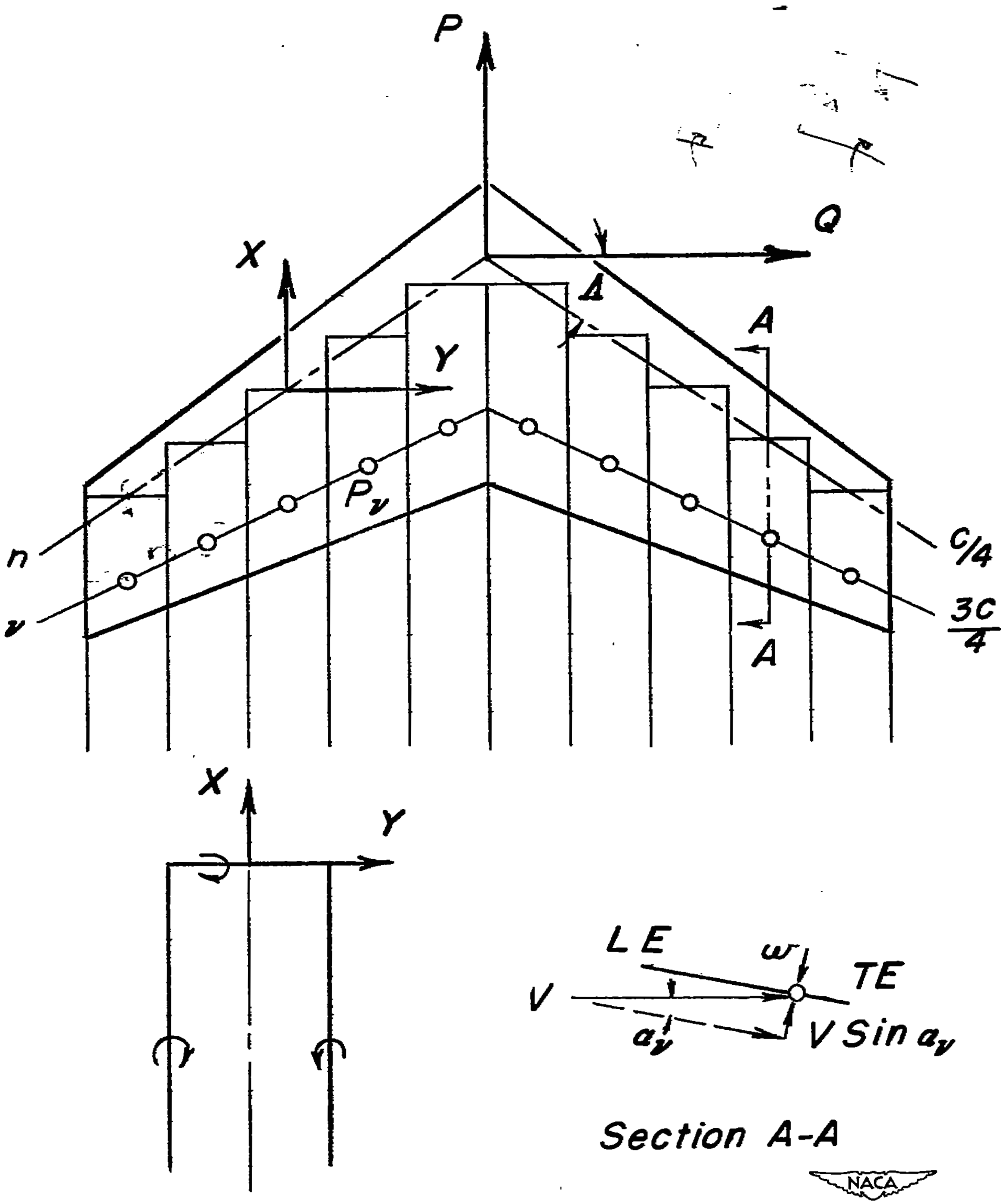

Figure 1.- Vortex pattern, system of axes, and subscripts used in calculation of span loadings by finite-step method (N = 10).

[redacted]

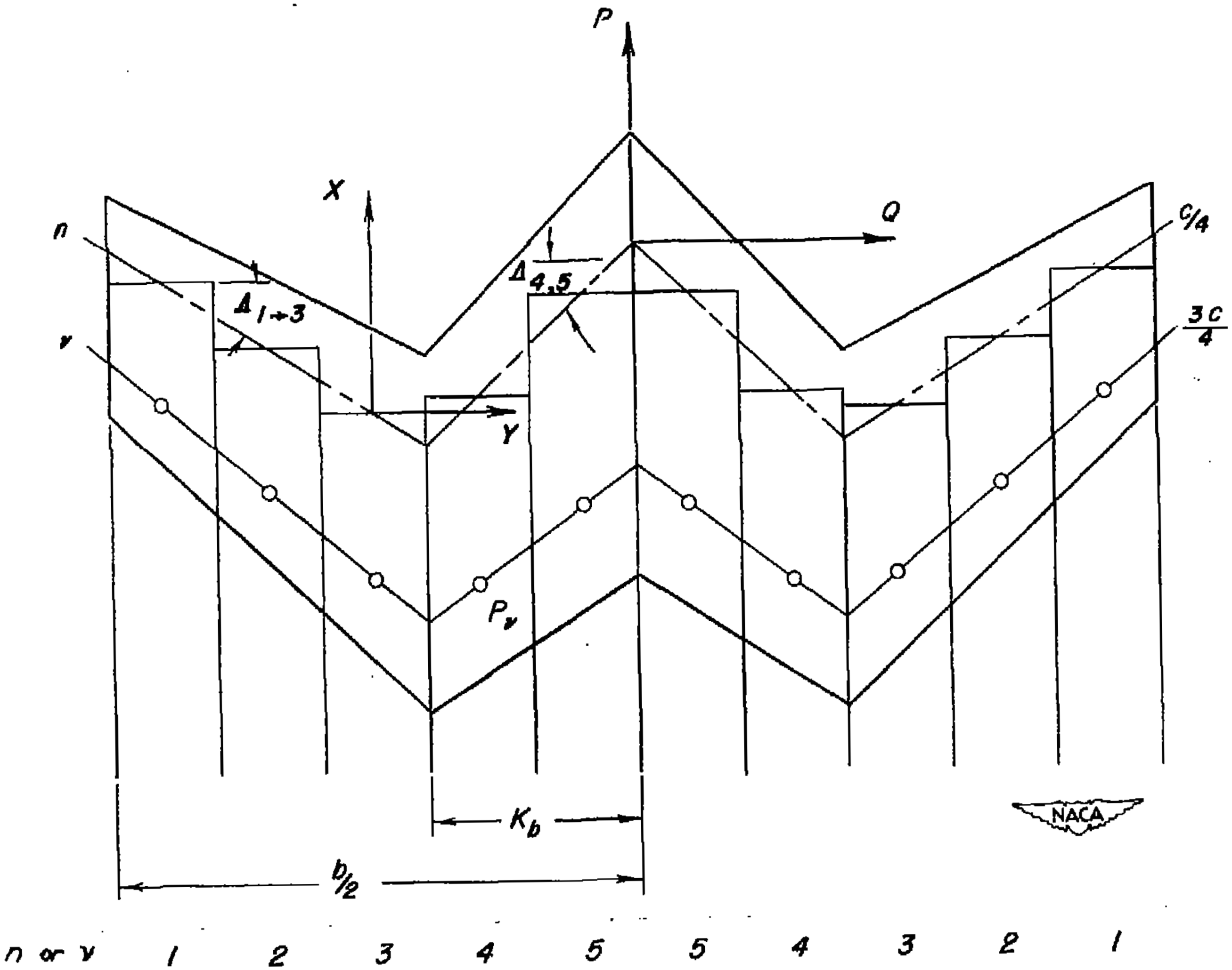

Figure 2.- Vortex pattern, system of axes, and subscripts used in calculation of span loadings by finite-step method; illustrated for W plan form (N = 10).

[redacted]

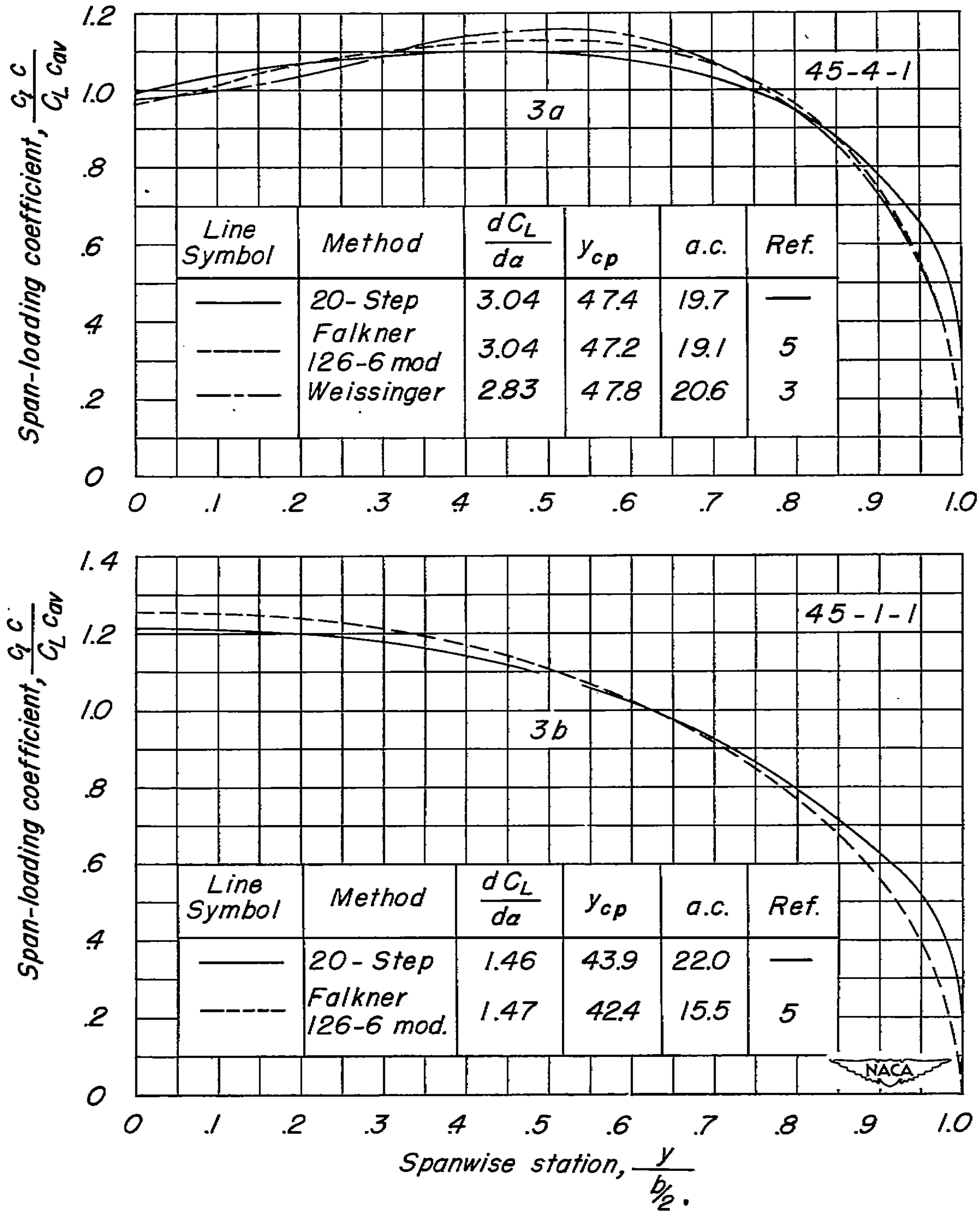

Figure 3.- A comparison of 20-step loadings with results of the Falkner and Weissinger methods.

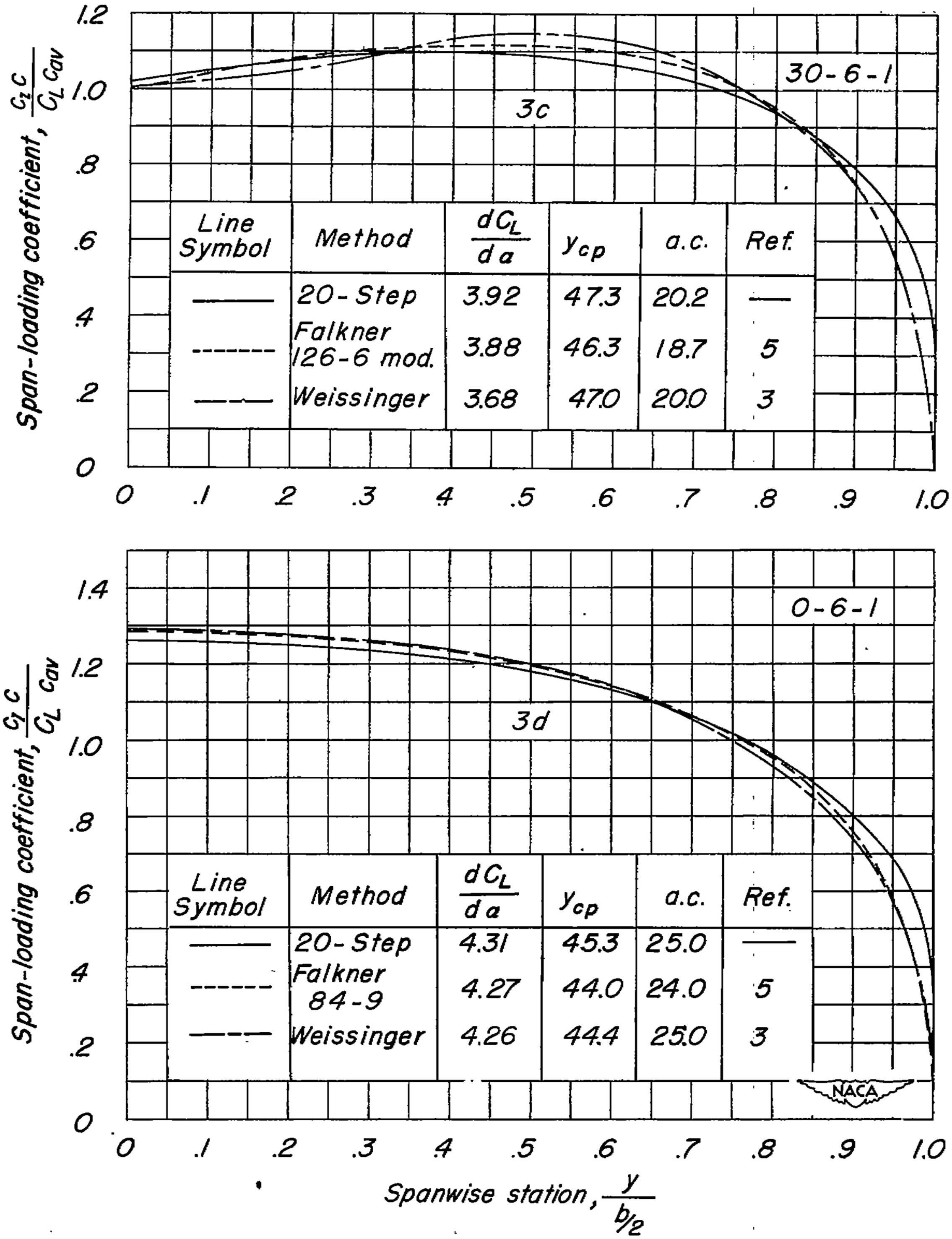

Figure 3.- Continued.

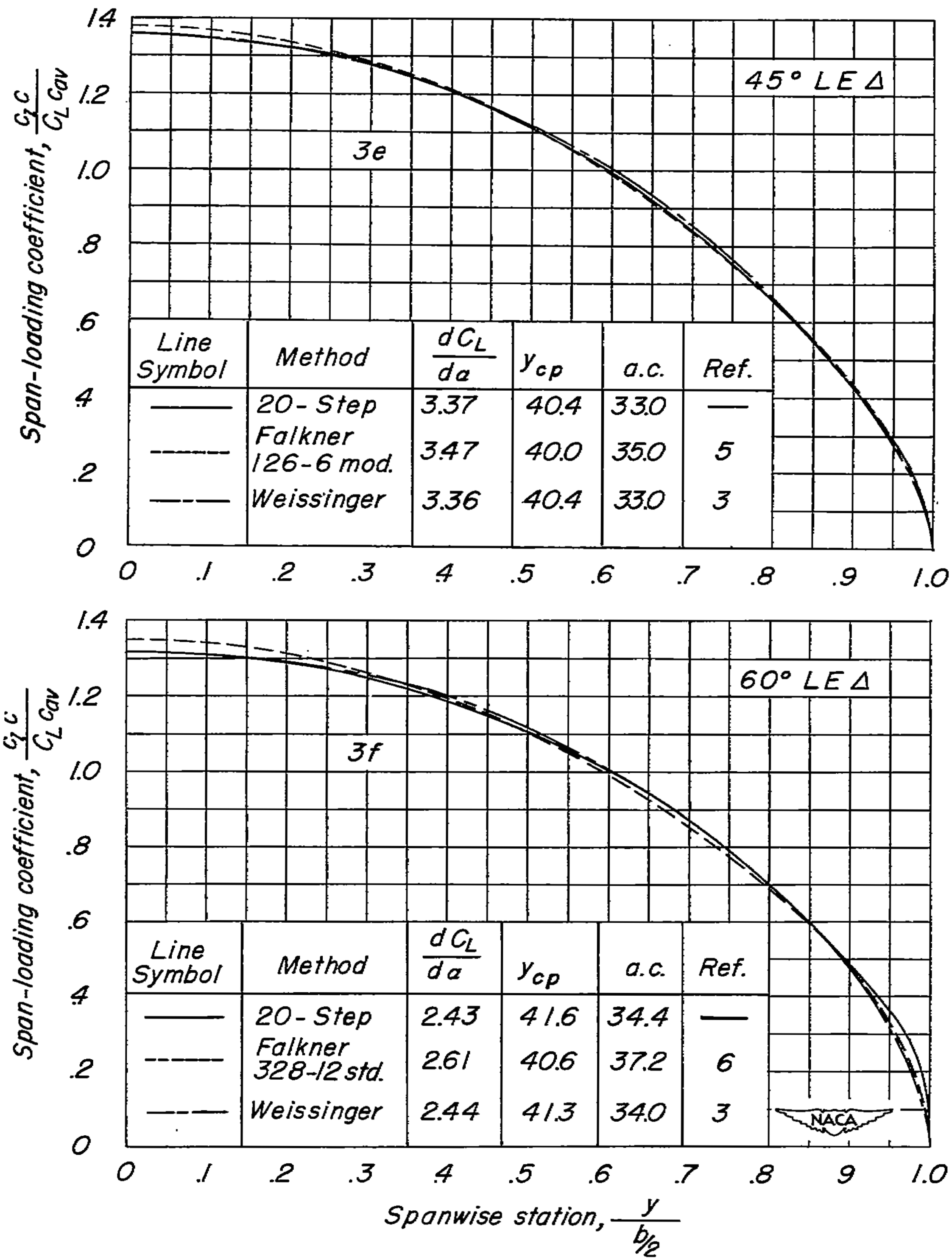

Line Symbol	Method	$\frac{dC_L}{d\alpha}$	y_{cp}	a.c.	Ref.
———	20-Step	3.37	40.4	33.0	—
- - - -	Falkner 126-6 mod.	3.47	40.0	35.0	5
— — —	Weissinger	3.36	40.4	33.0	3

Line Symbol	Method	$\frac{dC_L}{d\alpha}$	y_{cp}	a.c.	Ref.
———	20-Step	2.43	41.6	34.4	—
- - - -	Falkner 328-12 std.	2.61	40.6	37.2	6
— — —	Weissinger	2.44	41.3	34.0	3

Figure 3.- Concluded.

[redacted]

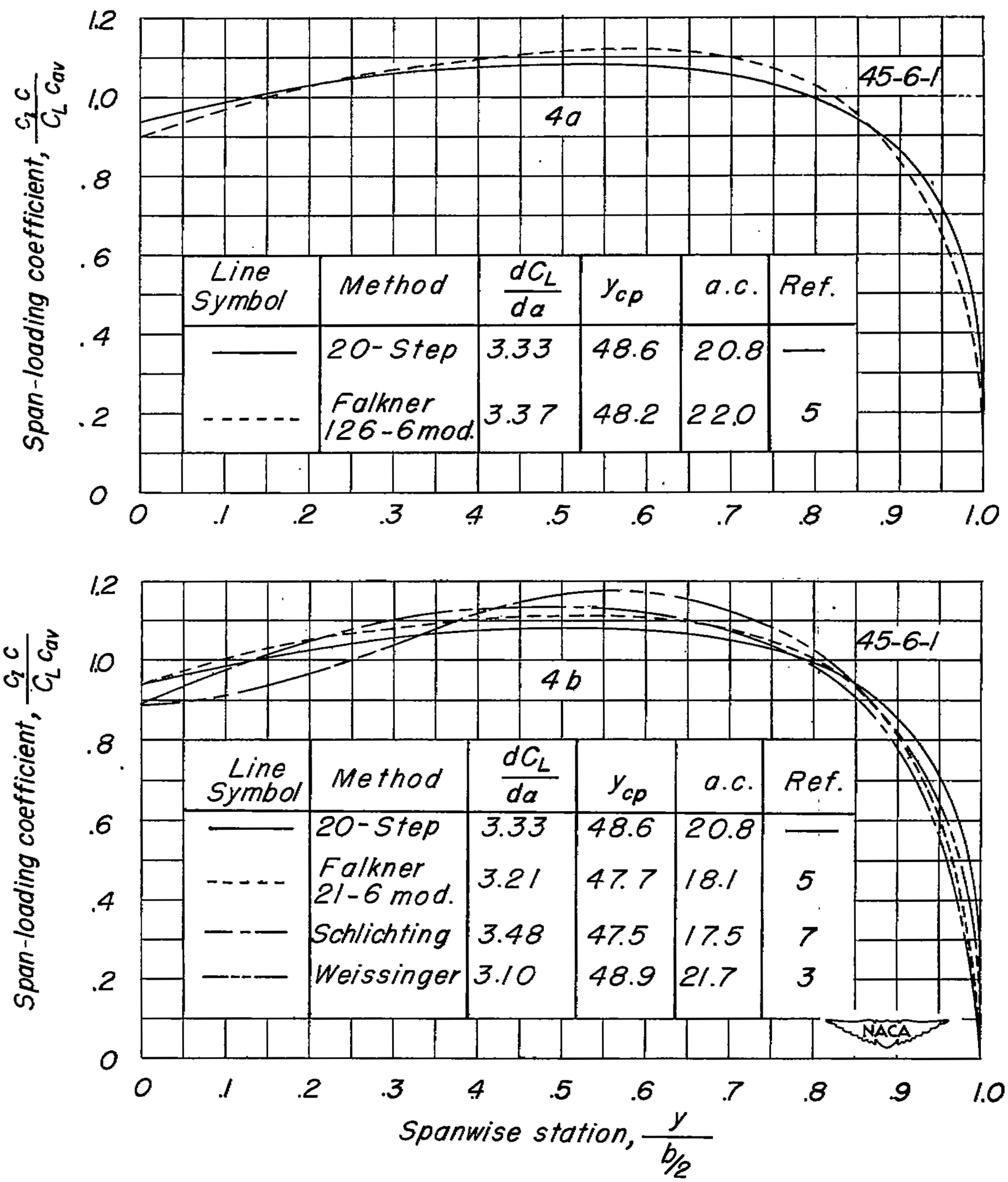

Figure 4.- Comparison of 20-step results with other methods for determining theoretical span loadings; untapered plan form of aspect ratio 6 and 45° sweepback.

[redacted]

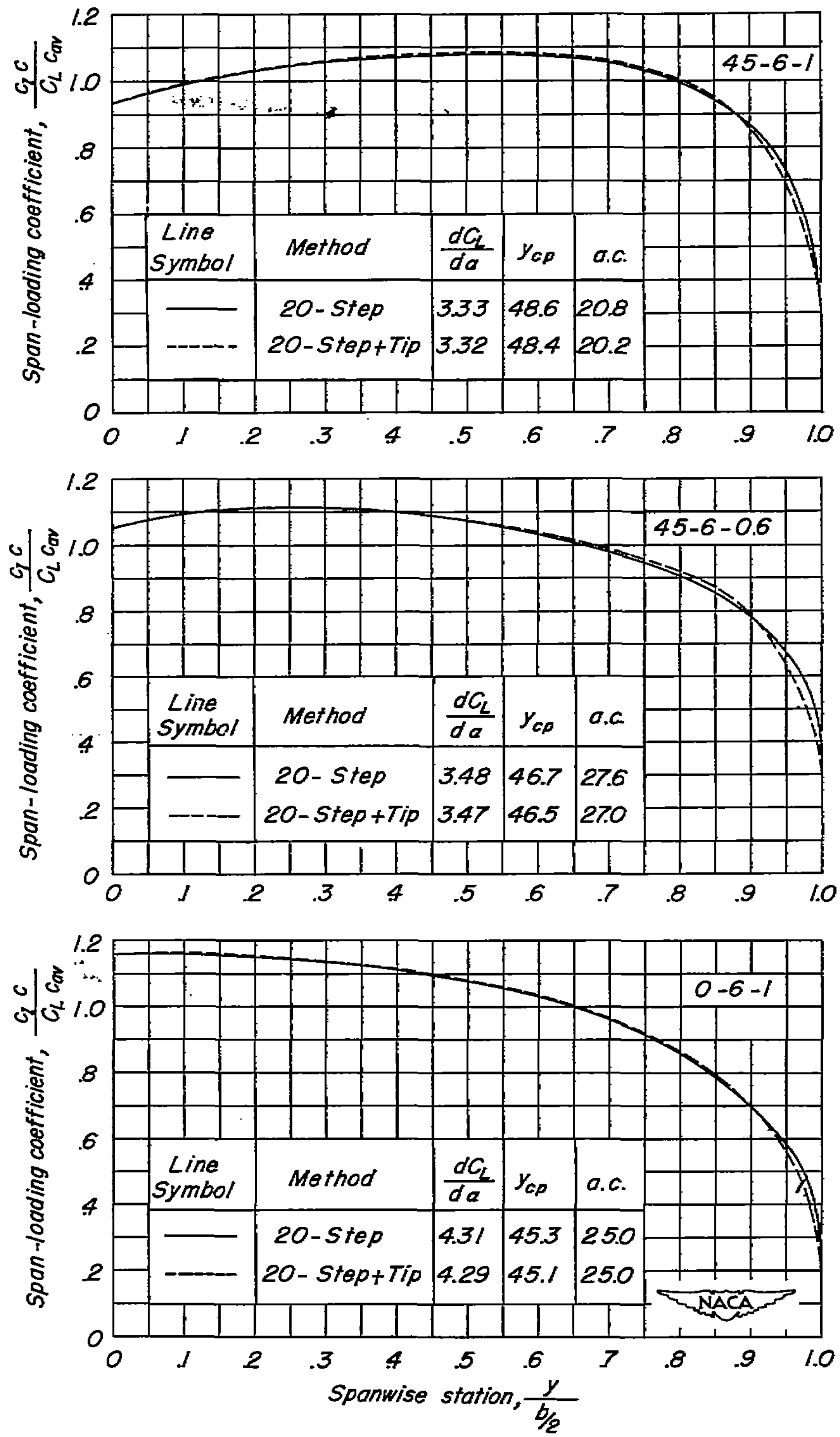

Figure 5.- The effect of an extra vortex located near the wing tip compared with 20-step results.

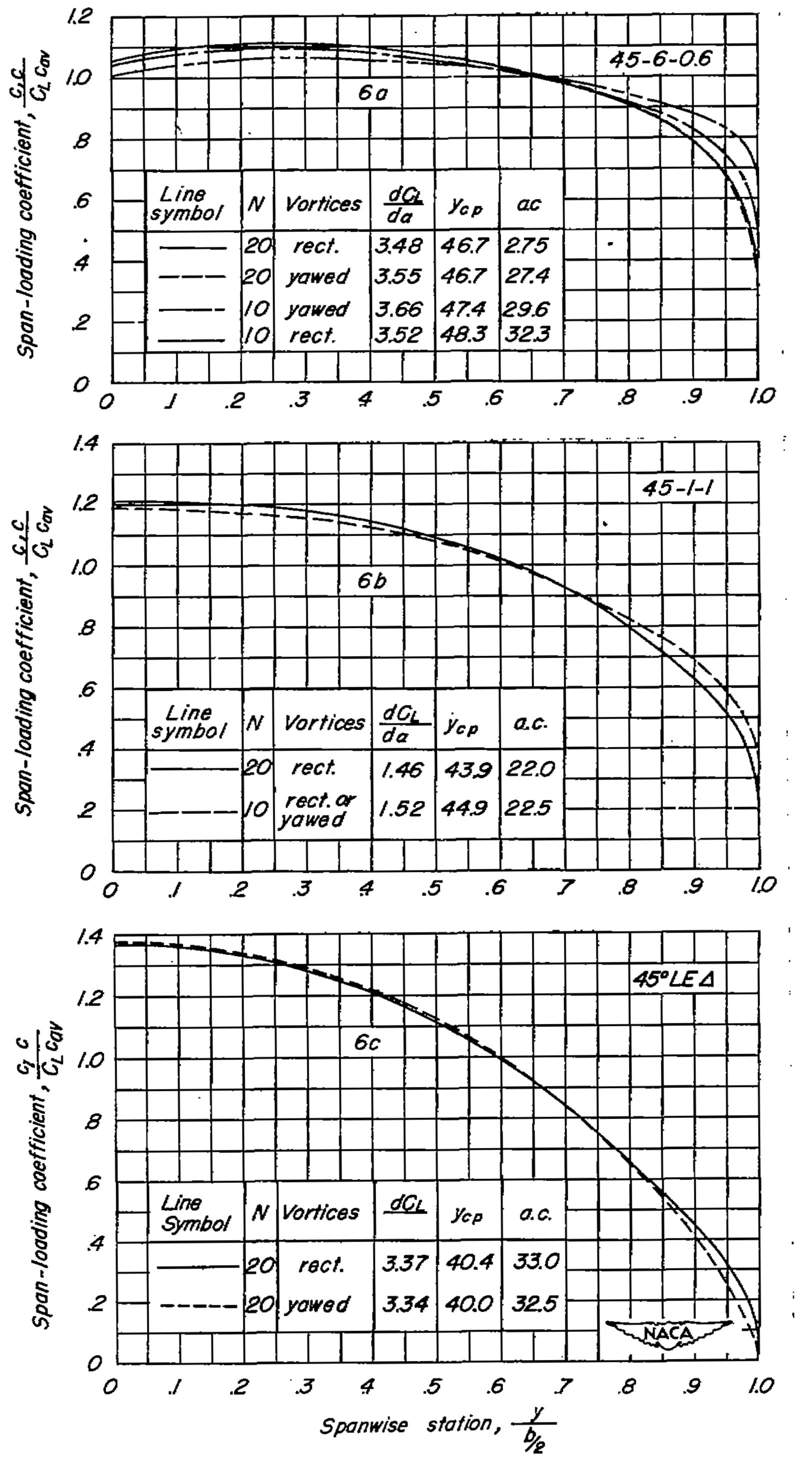

Figure 6.- Effect of yawed vortices and number of steps on span loading.

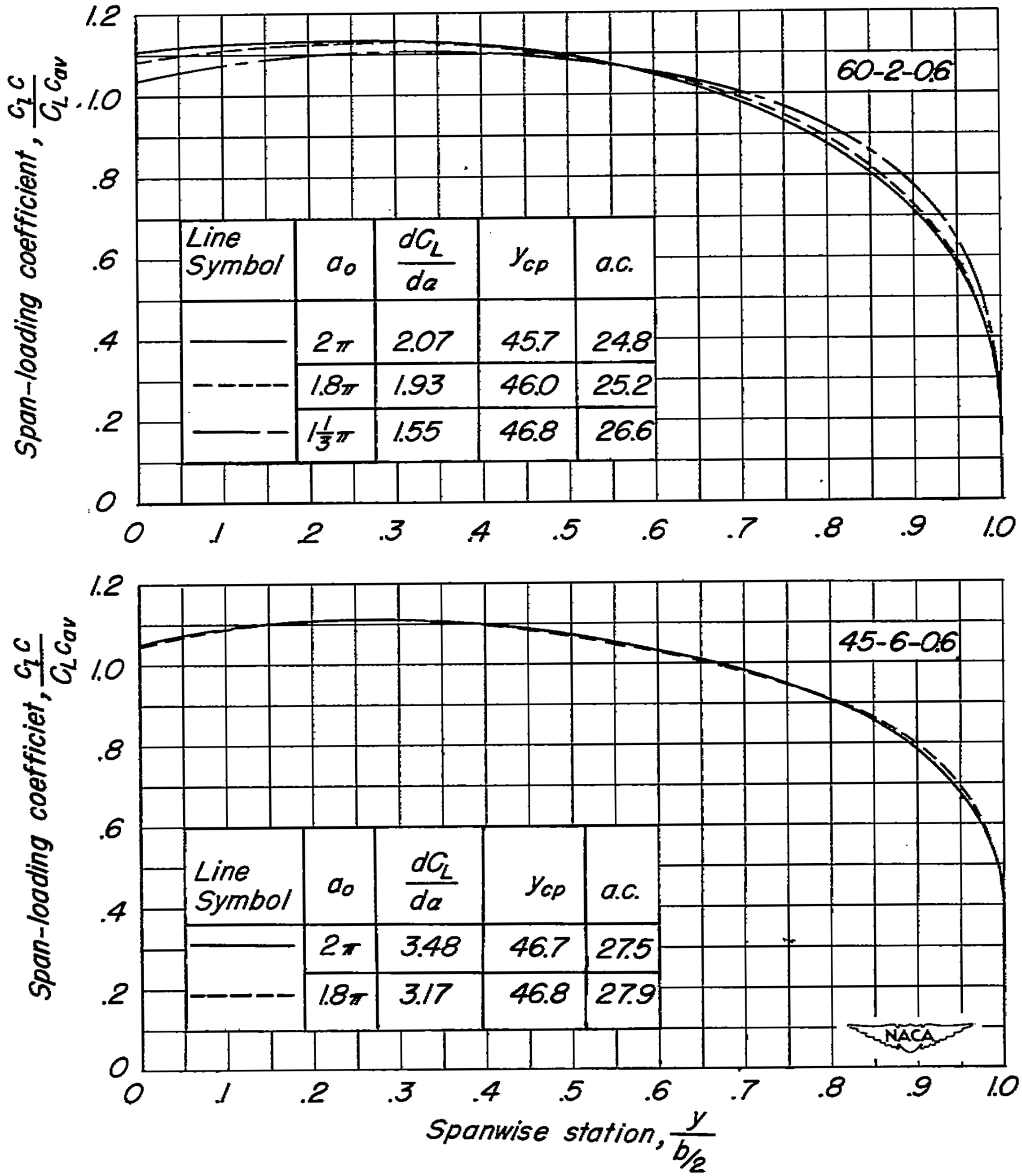

Figure 7.- Effect of section lift slope on span loading.

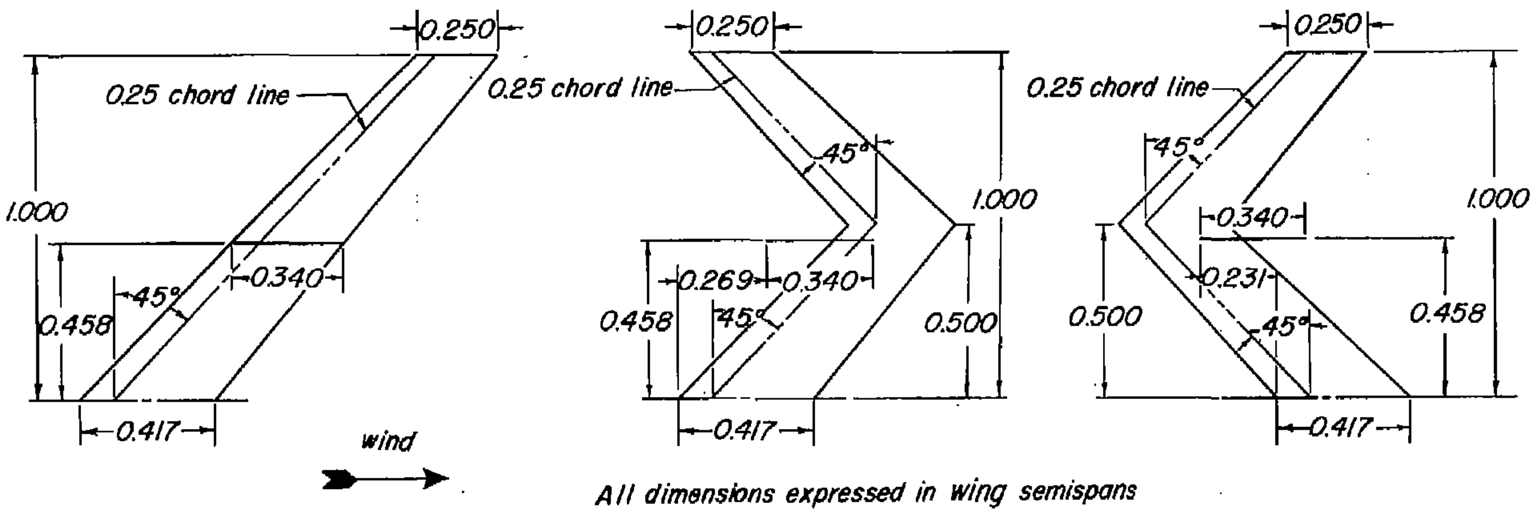

Tabulated Wing Data

Sweptback wing

Sweep	45°
Aspect ratio	6
Taper ratio	0.6

W-wing

Sweep of inboard panel	45°
Sweep of outboard panel	-45°
Aspect ratio	6
Taper ratio	0.6

M-wing

Sweep of inboard panel	-45°
Sweep of outboard panel	45°
Aspect ratio	6
Taper ratio	0.6

NACA

Figure 8.- Plan-form dimensions of sweptback, W-, and M-wings used as illustrative example.

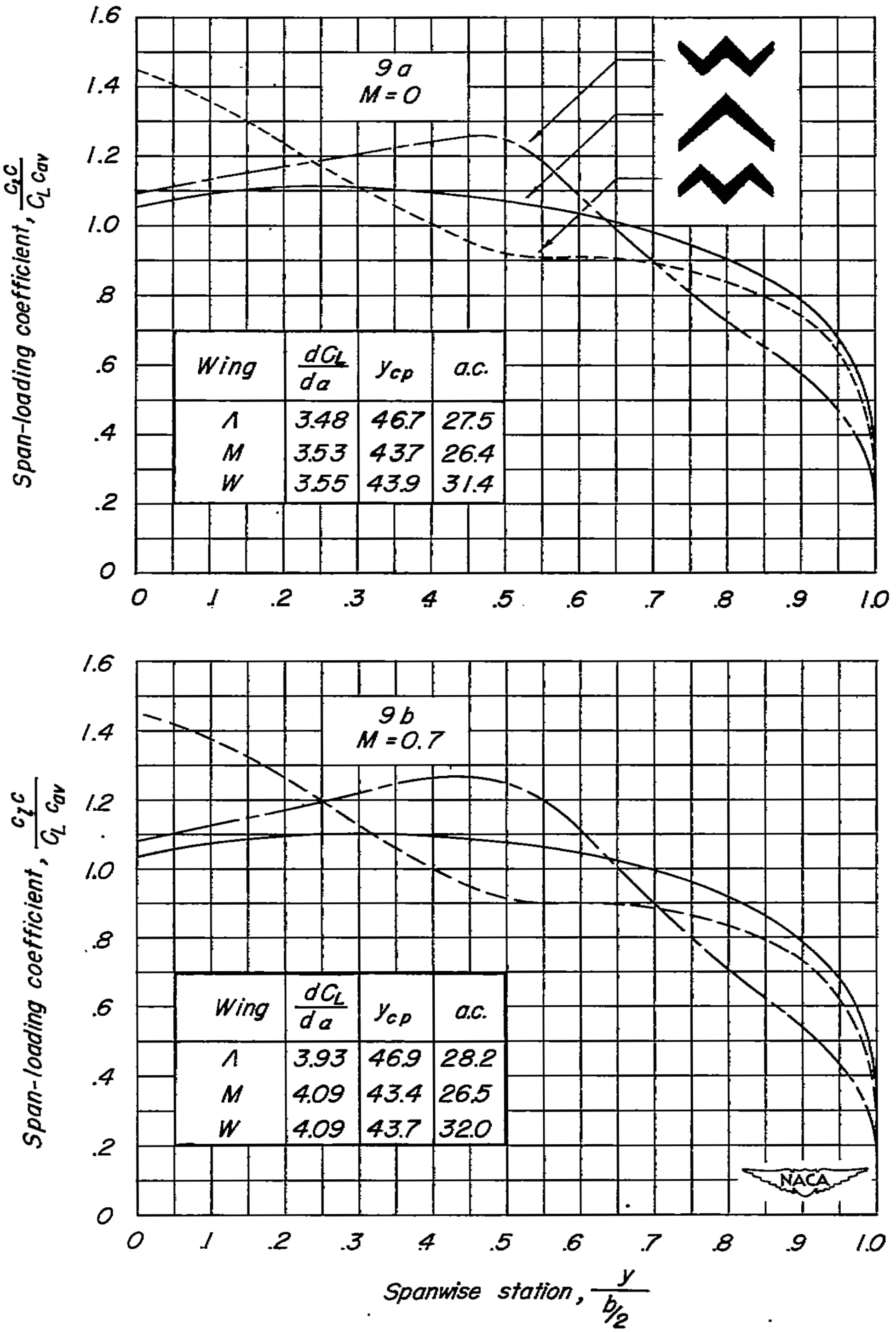

Figure 9.- Twenty-step loadings for sweptback, M-, and W-wings having 45° swept panels, aspect ratio 6, and taper ratio 0.6.

[redacted]

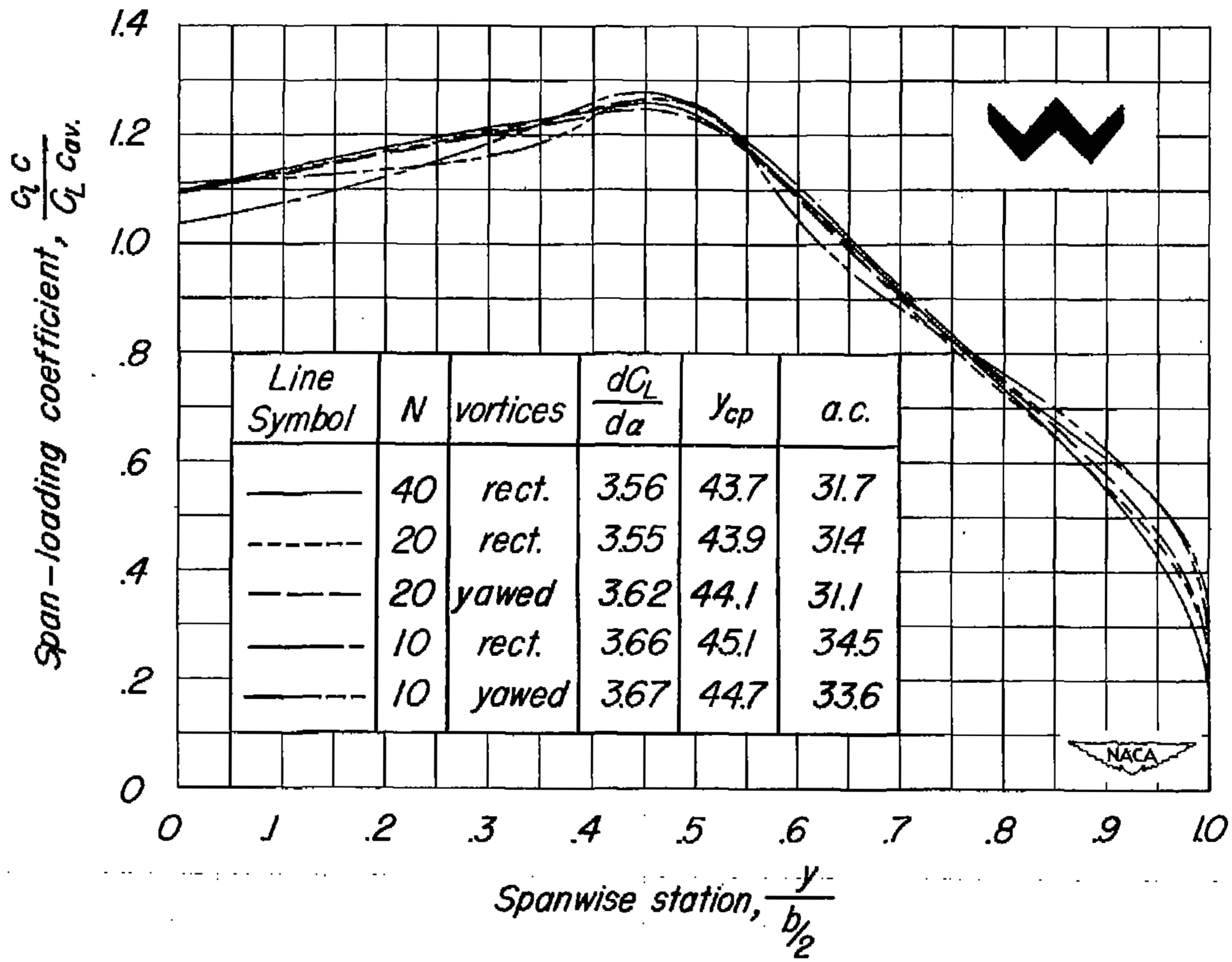

Figure 10.- Finite-step loadings for a W-wing having 45° sweptback panels, aspect ratio 6, and taper ratio 0.6.

[redacted]

~~CONFIDENTIAL~~ UNCLASSIFIED

UNCLASSIFIED

~~CONFIDENTIAL~~